AN ACTIVE FEEDBACK SYSTEM TO CONTROL SYNCHROTRON OSCILLATIONS IN THE SLC DAMPING RINGS*

P. L. CORREDOURA, J.-L. PELLEGRIN, H. D. SCHWARZ AND J. C. SHEPPARD
Stanford Linear Accelerator Center
Stanford University, Stanford, California 94305

1. Introduction

Initially the SLC Damping Rings accomplished Robinson instability damping by operating the RF accelerating cavities slightly detuned. In order to be able to run the cavities tuned and achieve damping for Robinson instability and synchrotron oscillations at injection an active feedback system has been developed. This paper describes the theoretical basis for the feedback system and the development of the hardware. Extensive measurements of the loop response including stored beam were performed. Overall performance of the system is also reported.

2. Feedback Model Development

To develop a reliable, well understood synchrotron feedback system, a mathematical model representing the system was developed. The approach was to use frequency domain methods which allowed classical feedback theory to analyze loop performance and stability.

Equation (1) is an energy balance equation modified to include a term for the feedback energy.[1] Feedback energy is the change in electron (or positron) energy produced by phase shifting the RF in the accelerating cavities.

$$\frac{d}{dT}\frac{\epsilon}{E_0} = \frac{1}{E_0 T_0}\left[U_0 + \Delta\phi e V_p \cos\phi_s - U_0 - 4U_0\frac{\epsilon}{E_0} + \Delta\phi_f e V_p \cos\phi_s\right] \quad (1)$$

where

- E_0 = steady state electron energy = ring design energy
- ϵ = energy deviation from E_0
- T_0 = time required for electron to orbit storage ring once
- U_0 = energy radiated each orbit = energy gained in RF cavities each orbit
- e = electron charge
- V_p = total peak gap voltage in RF cavities
- $\Delta\phi_f$ = phase shift imposed on RF accelerating field by the feedback system
- ϕ_s = synchronous phase of electron with respect to cavity RF
- $\Delta\phi$ = electron phase variations about ϕ_s

Relating phase deviations about ϕ_s to energy deviations[2] is Eq. (2)

$$\frac{d}{dT}\Delta\phi = -\omega_{RF}\alpha\frac{\epsilon}{E_0} \quad (2)$$

where

- ω_{RF} = frequency of storage ring RF, and
- α = momentum compaction factor.

The system differential equation is next derived from the coupled Eqs. (1) and (2). If one were to feed back with a signal proportional to the phase of the electron bunch one would eliminate the ϵ/E_0 term. Doing this shows that the resulting forcing function acts on the $\Delta\phi$ term of the resulting homogeneous equation. This would change the synchrotron frequency and not improve damping. One could, in theory, differentiate this signal for use in the feedback system but it is always desirable to keep differentiators out of feedback systems since they have increasing gain for increasing frequency and tend to add noise.

Feeding back with a signal proportional to the energy deviation requires the elimination of the $\Delta\phi$ terms in (1) and (2), resulting in

$$\ddot{\epsilon} + \frac{4U_0}{E_0 T_0}\dot{\epsilon} + \frac{\omega_{RF}\alpha\epsilon V_p\cos\phi_s}{E_0 T_0}\epsilon = \frac{\Delta\dot{\phi}_f e V_p \cos\phi_s}{E_0 T_0} \quad . \quad (3)$$

Since we are feeding back on a signal proportional to beam energy error

$$\Delta\phi_f = G K_\phi K_d \epsilon_f \quad (4)$$

where

- G = amplifier gain
- K_ϕ = phase shifter sensitivity
- K_d = energy detector sensitivity

Taking the derivative of (4) and substituting into (3) and grouping terms results in a homogeneous equation (5) with constant coefficients which describes a damped harmonic oscillator. The last term is the forcing function generated by the energy feedback. It is now obvious that the energy feedback acts on the $\dot{\epsilon}$ term which determines the rate of damping.

$$\ddot{\epsilon} + \frac{2}{T_\tau}\dot{\epsilon} + \omega_s^2\epsilon = -\frac{\omega_s G K_d}{\omega_{RF}\alpha}\dot{\epsilon}_f \quad (5)$$

where

- $1/T_\tau$ = damping time constant $= 2U_0/E_0T_0$
- ω_s = synchrotron frequency
  $= [(1/E_0T_0)\omega_{RF}\alpha e V_p \cos\phi_s]^{1/2}$

Taking the Laplace transform of (5) and solving for the ratio of $\epsilon(s)/\epsilon_f(s)$ gives us an open loop transfer function. Modifying this function to include the fill time effect of the RF accelerating cavity requires adding a first order pole to the transfer function. The calculation of the cavity fill time is as follows:

$$T_c = \frac{2Q_0}{\omega_{RF}(1+\beta)} \quad (6)$$

where

- Q_0 = Cavity unloaded Q = 26,800
- β = Cavity coupling factor = 2.46

The related pole frequency for the SLC damping ring cavities is 46 kHz.

Modifying the transfer function to include the effect of this new pole gives the desired open loop transfer function, $K(s)$

$$K(s) = \frac{\epsilon(s)}{\epsilon_f(s)} = -\left[\frac{\omega_s G K'_\phi K'_d}{\omega_{RF}\alpha}\right]\left[\frac{1}{T_c}\right]\left[\frac{s}{s^2 + (2/T_\tau)s + \omega_s^2}\right]\left[\frac{1}{s + (1/T_c)}\right] \quad . \quad (7)$$

Using the open loop transfer function (7) a root locus plot can be made to determine system stability. A system with open loop response described by the transfer function K(s) has a closed loop response T(s) related to K(s) as follows

$$T(s) = K(s)/(1 + K(s)) \quad . \quad (8)$$

Instability is related to the roots of 1 + K(s) = 0. For zero gain these roots are situated at the poles of K(s), but as the gain is increased they follow a contour which leads them to the zeroes of K(s). Making a root locus plot of (7) revealed that we did indeed have a stable system but could only decrease the damping time by a factor of two. For further improvement additional compensation was required. Lead compensation was designed into the feedback amplifier which effectively removed the pole caused by the cavity fill time. The resulting root locus plot (Fig. 1) shows that for increasing gain, damping time decreases until critical damping is reached. This is the desired result.

3. Hardware Development

Once it was established that an energy error detector was to be used to provide the feedback error signal, a suitable detector had to be developed. Energy error is related to the radial position of the beam through the momentum compaction factor and the amount of dispersion where the beam position is measured.

The chosen energy error detector (Fig. 2) is composed of several parts. Two stripline Beam Position Monitors (BPM) electrodes produce impulses induced by the beam with amplitudes proportional to the electrode distance from the beam and also to the beam intensity. The individual BPM strips used are on opposite sides of the beam pipe but are skewed 45° below the horizontal plane. This topology reduces heating by beam interception and synchrotron radiation interception. The impulses from the two BPM electrodes travel 80 meters through low-loss coaxial cables into two separate envelope detectors.

* Work supported by the Department of Energy, contract DE-AC03-76SF00515.

CH2669-0/89/0000-1879$01.00©1989 IEEE

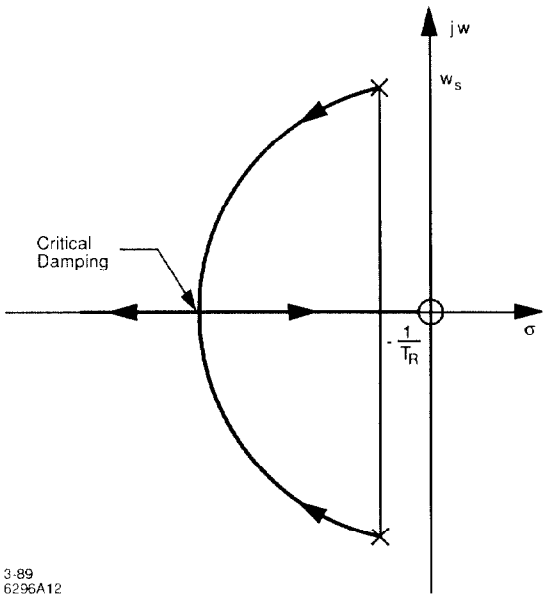

Fig. 1. Root locus plot of the feedback system.

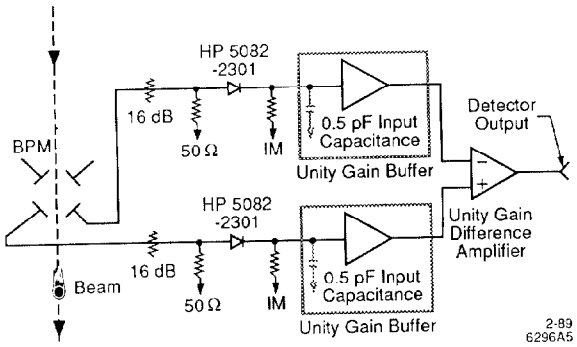

Fig. 2. Energy error detector schematic.

Each envelope detector consists of an attenuator, termination, hot carrier detector diode, charge storage capacitance, bleed off resistor and output buffer. The attenuator is selected to provide a 10 V peak impulse when 5×10^{10} electrons are stored. The diode conducts when the impulse voltage exceeds the voltage stored in the capacitance. The bleed off resistor allows the stored voltage to drop at a rate which slightly exceeds the maximum slew rate of the synchrotron signal. Each envelope detector is buffered with a high input impedance unity gain buffer.

The output of each envelope detector is subtracted in a unity gain differential amplifier. Taking the difference increases the detectors horizontal sensitivity while reducing vertical sensitivity. The resulting signal is proportional to radial beam position and beam intensity. The effect of increasing beam intensity is to increase the sensitivity of the detector and in turn increasing the loop gain. This results in decreasing the damping time of the synchrotron oscillations.

The next component loop is the feedback amplifier (Fig. 3). The amplifier not only provides an adjustable loop gain but also compensates for the first order pole introduced by the cavity fill time. A zero in the frequency response placed at 45 kHz cancels the cavity pole. The pole associated with this compensation is at 8 MHz and does not affect the loop performance. A wide band current mode operational amplifier was used for the feedback amplifier to minimize phase shift as the loop gain was varied.

The output of the feedback amplifier drives an electronic phase shifter.[3] The phase shift across the device is linearly proportional to the applied control voltage. A 10 V change in the control voltage produces a 180° phase shift. The phase shifter used for the synchrotron feedback loop is fast enough to allow modulation frequencies of several MHz. This insured that the loop dynamics at the synchrotron frequency would not be altered by additional poles. The phase shifter is located in the drive line to the klystron which, in turn, supplies the power for the RF accelerating field in the cavities.

The UHF klystron has a specified bandwidth of 10 MHz. As with the phase shifter, the poles associated with the klystron are two decades above the synchrotron frequency and do not effect the feedback loop.

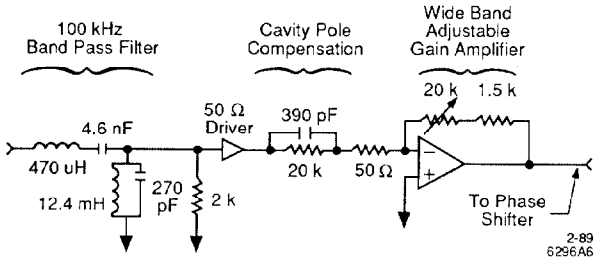

Fig. 3. Feedback amplifier schematic.

A bandpass filter was added to the system to insure that low frequency components of the feedback signal would not interfere with an existing beam extraction phase feedback system and also to reduce high frequency system noise. The filter was designed to have a flat phase and amplitude response over nearly two decades centered at the 100 kHz synchrotron frequency.

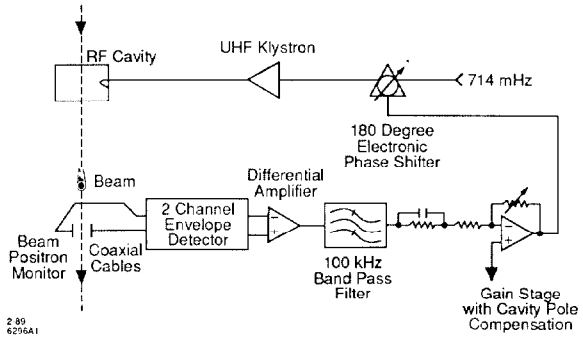

Fig. 4. System block diagram figure.

Each major component of the feedback system has now been described. Figure 4 shows the system configuration.

4. Loop Testing Methods

The response of various sections of the loop in the frequency domain was measured and compared to the predicted response from the model. Measurements were made with a HP 3577A low frequency network analyzer, data was recorded in the form of Bode plots. A fortran program was written to produce Bode plots based on the loop model which could be directly compared to the measured loop responses.

To measure the RF cavity response the network analyzers swept reference signal was applied to the phase shifter in the drive to the klystron. The resulting variations in the cavity field were measured by a phase detector monitoring the phase across the cavity. The response of the klystron and the phase shifter is imbedded in this measurement and all subsequent down stream measurements. Since their associated pole frequencies are nearly two decades above the synchrotron frequency, they do not affect our measurements up to a decade above the synchrotron frequency.

The response of the beam itself could only be measured with the help of the RF system to modulate the beam energy and the energy error detector to measure the response. So both the cavity response and the energy error detector response are imbedded in the overall beam response measurement. Since the response of the cavity and drive system was already known, the response of the beam and the detector could be extracted from the measurement. Knowing the form of the beam response allowed the final extraction of the energy error detectors response.

The frequency response of the feedback amplifier and the bandpass filter were also measured. The frequency of the zero in the amplifiers response and the flat phase response of the filter were verified.

The total open loop response was measured by applying the swept reference frequency to the klystron drive phase shifter while the measured signal was simply the output from the feedback amplifier. By using the described measurement procedures, some unexpected problems were identified.

5. System Test Results

The response of the prototype energy error detector was tested on the damping ring with a stored beam. The measured data did not match what our model had predicted. The measurements did show the expected zero at DC, the first order cavity pole at 45 kHz, and the second order beam resonance at the synchrotron frequency. Additionally an other pole and an exponentially increasing phase lag appeared near the synchrotron frequency.

The additional pole was traced to the energy error detector. The effective impedance of the hot carrier diode driven by the BPM impulses was measured to be 47 kΩ. This impedance is a function of the diode inductance and video resistance. The charge storage capacitance initially used was about 20 pF. This capacitance and the diode impedance created a pole in the response at 170 kHz, very close to the synchrotron frequency. In the next version of the detector the .5 pF input capacitance of the unity gain buffer amplifier became the charge storage element. The layout of the detector was optimized to minimize parasitic capacitance. These modifications moved the pole associated with the detector up to about 6 MHz.

The exponentially increasing phase lag was due to system delay. The electronics for the feedback system is located about 80 meters from the damping rings. The cable delays alone added 20° of phase lag at 100 kHz. To help compensate for this the zero in the amplifier response was moved down from 45 kHz to 20 kHz. In the future it is planned to relocate the RF stations directly over the damping rings, which will substantially reduce the amount of system delay.

With the above modifications made to the hardware and the delay element added to the model, good correlation between the model and the measured total open loop response was obtained (Fig. 5).

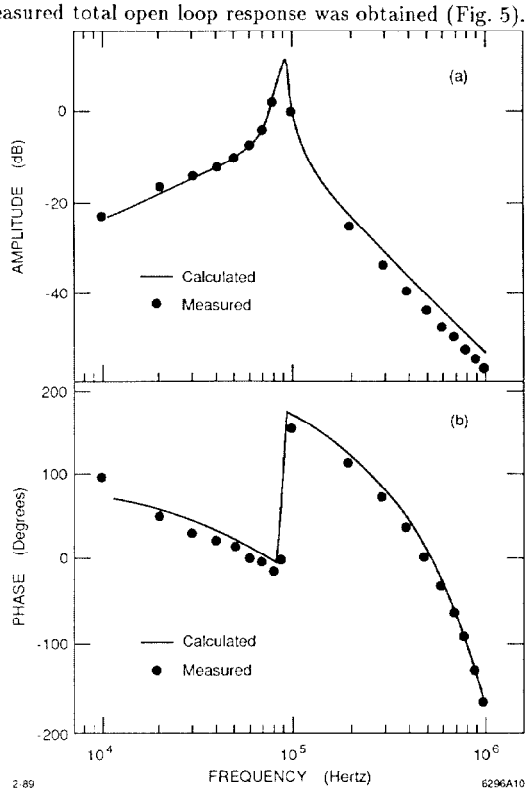

Fig. 5. Cavity, beam and energy error detector response.

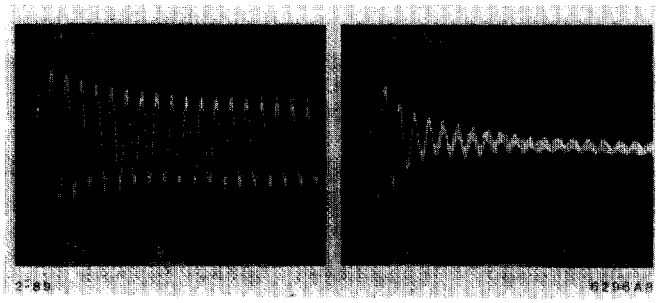

Fig. 6. Synchrotron oscillations at injection. Loop open and loop closed.

At this point the feedback loop was closed and the effect on the damping time of the synchrotron oscillations was measured. Figure 7 shows that the damping time could be reduced dramatically. Detuning of the RF accelerating cavities was no longer necessary to control Robinson's instability. Operating the cavities at resonance increased the amount of attainable gap voltage by 15%, related to the cosine of the previous detuning angle of 30°.

It was found that if the gain was raised to the point of critical damping, the beam would become unstable 1 to 2 ms after the initial synchrotron oscillations were damped. The cause of this phenomenon is not understood at the present time but may be related to the substantial amount of system delay reducing our phase margin. Presently the loop is operated at a lower gain which controls the oscillations without the instability problem.

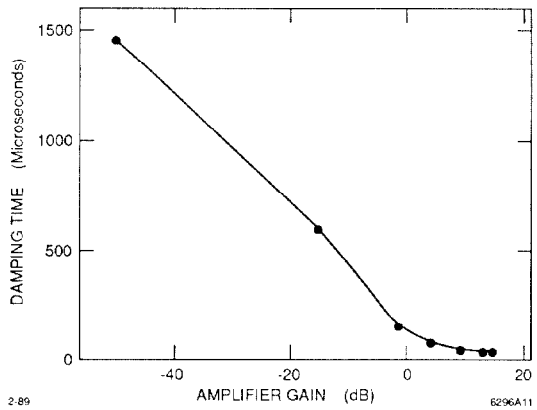

Fig. 7. Damping time versus gain figure.

References

1. M. Sands, "The Physics of Electron Storge Rings, An Introduction." SLAC-Report-121 (Eq. 3.34), November 1970.
2. *Ibid,* (Eq. 3.32).
3. J.-L. Pellegrin, H. D. Schwarz, "Control Electronics of the PEP RF System," IEEE, NS-28, No. 3, pp 2320, June 1981.